Energy 126 (2017) 622–637

Contents lists available at ScienceDirect

Energy

journal homepage: www.elsevier.com/locate/energy

Demand side management in a smart micro-grid in the presence of renewable generation and demand response

G.R. Aghajani [a, *], H.A. Shayanfar [b], H. Shayeghi [b, c]

[a] Department of Electrical Engineering, Science and Research Branch, Islamic Azad University, Tehran, Iran
[b] Centre of Excellence for Power System Automation and Operation, Department of Electrical Engineering, Iran University of Science and Technology, Tehran, Iran
[c] Technical Engineering Department, University of Mohaghegh Ardabaili, Ardabil, Iran

ARTICLE INFO

Article history:
Received 9 September 2015
Received in revised form
17 November 2016
Accepted 12 March 2017

Keywords:
Smart microgrid
Renewable generation
Demand side management
Demand response program

ABSTRACT

In this study, a stochastic programming model is proposed to optimize the performance of a smart micro-grid in a short term to minimize operating costs and emissions with renewable sources. In order to achieve an accurate model, the use of a probability density function to predict the wind speed and solar irradiance is proposed. On the other hand, in order to resolve the power produced from the wind and the solar renewable uncertainty of sources, the use of demand response programs with the participation of residential, commercial and industrial consumers is proposed. In this paper, we recommend the use of incentive-based payments as price offer packages in order to implement demand response programs. Results of the simulation are considered in three different cases for the optimization of operational costs and emissions with/without the involvement of demand response. The multi-objective particle swarm optimization method is utilized to solve this problem. In order to validate the proposed model, it is employed on a sample smart micro-grid, and the obtained numerical results clearly indicate the impact of demand side management on reducing the effect of uncertainty induced by the predicted power generation using wind turbines and solar cells.

1. Introduction

Future distribution systems will certainly face the increased penetration of wind and solar renewable sources, which have an intermittent natural behavior. This may endanger the security of the system operation [1,2]. In order to implement advanced planning for Distributed Energy Resources (DERs) to ensure the economic and safe operation of these systems, and Advanced Measuring Infrastructure (AMI) is necessary [3–5]. AMI establishes a bidirectional telecommunication between customers and electricity companies to provide readability, monitoring, and remote control of meters; data collection and transmission to electricity companies; processing and analysis of information, as well as the implementation of energy consumption management in an attempt to ensure the reliability of the system and to guarantee the creation of a balance between supply and demand [6–8].

To manage and control a smart microgrid, the structure of the AMI system generally includes:

- Smart meters with Power Line Carrier (PLC) communications installed at the customer premises. The smart meter of medium and large customers using General Packet Radio Service (GPRS) could be directly connected to the utility.
- To manage all smart meter measured data from each installation, Data Concentrators (DC) are installed in the proximity of 20 kV/400 V distribution transformers. Data concentrators integrate PLC communications that exchange information with smart meters and communicate with central.
- Meter Data Management Systems (MDMSs) are mainly Meter Data Management & Repository (MDM/R) systems in which the received unprocessed data are collected from all meters or sensors then processed in order to deliver the required data to distributed system operator and application systems.

One of the main drawbacks in the management of renewable resources, including wind and solar energies, is the issue of uncertainty in their behavior, such that before the use of solar and wind energy and other renewable energies in power system,

* Corresponding author. Basij Sq, Ardabil, Iran. Tel./fax: +98 4533513957.
E-mail address: aghajani__gholamreza@yahoo.com (G.R. Aghajani).

http://dx.doi.org/10.1016/j.energy.2017.03.051
0360-5442/

Nomenclature

r	total number of residential consumers
c	total number of commercial consumers
i	total number of industrial consumers
η	efficiency of the PV system
Si	solar irradiance(kW/m^2)
Pr_s	probability of scenarios
α_w	scale parameter Weibull distribution
β_w	shape parameter Weibull distribution
V_{wind}	wind speed(m/s)
V_m	average wind speed
P_R	rated power of the wind turbine
V_{ci}	cut-in speed of the wind turbine
V_r	rated speed of the wind turbine
V_{co}	cut-in speed of the wind turbine
$f_v(V_{wind})$	wind speed probability density function
$F_v(V_{wind})$	wind speed distribution function
$P_w(V_{wind})$	power output of WECS(kW)
$f_{P_w}(P_w)$	probability density function for the power output of WECS
$f_{P_{PV}}(si)$	solar irradiance probability density function
$F_{P_{PV}}(si)$	solar irradiance distribution function
$P_{PV}(si)$	power output of PVS
P_h	power output of HSWPS
$f_h(P_h)$	probability density function for the power output of HSWPS
RC(r,t)	amount of load reduction planned by each residential consumer in period *t*
CC(c,t)	amount of load reduction planned by each commercial consumer in period *t*
IC(i,t)	amount of load reduction planned by each industrial consumer in period *t*
RC_t^{max}	maximum load reduction proposed by each residential consumer in period *t*
CC_t^{max}	maximum load reduction proposed by each commercial consumer in period *t*
IC_t^{max}	maximum load reduction proposed by each industrial consumer in period *t*
$\zeta_{r,t}$	amount of incentive payment to each residential consumer in period *t*
$\zeta_{c,t}$	amount of incentive payment to each commercial consumer in period *t*
$\zeta_{i,t}$	amount of incentive payment to each industrial consumer in period *t*
F^{Cost}	total expected cost
$F^{Emission}$	total emissions
COC(t)	certain operational cost function
UOC(t)	uncertain operational cost function
$P_i(t)$	output power *i*th unit in period *t*
$\pi_i(t)$	offered price *i*th unit in period *t*
$I_i(t)$	on and off status of the *i*th DG in period *t*
$SU_i(t)$	start up or shut down cost of the *i*th DG in period *t*
$RC_i^{DG}(t)$	reserve costs of the *i*th DG in period *t*
$RC_j^{DR}(t)$	demand response program coats of the *j* th load in period *t*
$P_{Grid}(t)$	active power bought/sold from/to the utility in period *t*
$\pi_{Grid}(t)$	offered price bought/sold from/to the utility in period *t*
$C_{i,s}^{DG}(t)$	running cost of the *i*th DG unit at the *t* th period in the *s*th scenario
$C_{j,s}^{DR}(t)$	the cost caused by load reduction by the *j* th DRPs during the *t* th period in the *s*th scenario
$ENS_{n,s}(t)$	amount of involuntarily load shedding in period *t* and scenario *s*
$Emi_{DG}(t)$	average pollution of DG units
$Emi_{Grid}(t)$	average pollution of Grid
$CO_{2,i}(t)$	carbon dioxide pollutants of *i*th DG unit in period *t* (kg/MWh)
$SO_{2,i}(t)$	sulfur dioxide pollutants of *i*th DG unit in period *t* (kg/MWh)
$NO_{x,i}(t)$	nitrogen oxide pollutants of *i*th DG unit in period *t* (kg/MWh)
$P_{Demand_{t,s}}$	load consumption in period *t* and scenario *s*
$P_{DR,s}(t)$	active power participated in DPRs
$R_{DG}(i,t)$	scheduled spinning reserve provided by DG I in period t
$P_{DG}(i,t,s)$	active output power of DG I in period t and scenario s
$P_{DG,i}^{min}$	minimum output power limit of DG i
$P_{DG,i}^{max}$	maximum output power limit of DG i
$W_{ess}(t)$	battery energy storage at time *t*
$\eta_{charge}(\eta_{discharge})$	charge(discharge) efficiency of the battery

List of abbreviations

PDF	Probability Density Function
CDF	Cumulative Distribution Function
DRP	Demand Response Program
DSM	Demand Side Management
DER	Distributed Energy Resource
AMI	Advanced Metering Infrastructure
DR	Demand Response
PSO	Particle Swarm Optimization
MOPSO	Multi-Objective Particle Swarm Optimization
WES	Wind Energy System
PLC	Power Line Carrier
DC	Data Concentrators
MDM/R	Meter Data Management & Repository
PVS	Photovoltaic System
PVS	Photovoltaic System
HSWPS	Hybrid Solar-Wind Power System
DG	Distribution Generation
VOLL	Value of Lost Load
EENS	Expected Energy Not Served
MT	Micro-Turbine
WT	Wind Turbine
PV	Photovoltaic
FC	Fuel Cell
PCC	Point of Common Coupling
GPRS	General Packet Radio Service
MDMS	Meter Data Management System

network operators have always used storage services to manage production shortages and to create a balance between production and consumption. Today, with the advent of renewable energies, such as wind and solar energy, and the lack of certainty in their production potential, the need to provide storage and find a solution to resolve this uncertainty is felt more than ever. One of these solutions is the use of Demand Response Programs (DRPs) [9,10].

Recently, significant studies have been conducted for better implementation of demand side management programs and modeling their roles in creating a balance between generation and consumption in the presence of renewable generation, considering their stochastic behavior. Demand response programs were used in Ref. [11] to manage the operation of a smart micro-grid with wind and solar resources, and Particle Swarm Optimization (PSO) algorithm was applied to solve the proposed model so that the pollution emission function was not considered in modeling the micro-grid management. Multi-objective operation planning in a smart distribution grid with wind and solar resources was evaluated in Ref. [12] as a probabilistic model to reduce operational costs and emissions; Rayleigh and beta Probability Density Functions (PDFs) were used for modeling variations in the wind speed and solar radiation, respectively. In this reference, simultaneous modeling of solar and wind power generation is not considered, and on the other hand, the definition of pollution function from elements such as SO_2 and NO_x is ignored, and the ε-constraint method is used for problem-solving. A similar problem was discussed by Zakariazadeh et at. in Ref. [13], where a scenario tree approach was used to solve the problem; in this study, authors have ignored solar power modeling.

Online optimal management and modeling of a micro-grid with poly-generation were studied in Ref. [14] the using mesh adaptive direct search method in which the uncertainty caused by renewable generation was ignored. In Ref. [15], using demand response programs was proposed for controlling the frequency of a smart microgrid with renewable generation. A multi-objective function has become a single objective function, and Mixed Integer Liner Programming (MILP) method is used to solve the proposed model.

The use of demand side management in a smart grid, considering the wind power generation (wind farm) and the resulting uncertainty, was studied by Cicke et al. in Ref. [16] in order to increase social welfare. In this research, the authors don't consider the use of solar power generation and do not use incentive-based demand response programs that can cause consumers the motivation to participate. Using a stochastic planning approach based on the Monte Carlo method was suggested in Ref. [17] for modeling the stochastic behavior of wind and Demand Response (DR) considering the influence of wind power as an operational storage in an energy market.

This paper aims to find the optimal operation of the smart microgrid with the purpose of minimizing operational costs and emissions and considering the concept of DR in smart grids for covering the uncertainty caused by wind and solar power generation and taking into account the stochastic natural behavior. Since consumer's participation in these programs is considered to be completely voluntary, an incentive-based demand response method is proposed for implementing demand response programs. In this method, programs are considered in the form of offering packages of price and storage of DR for residential, commercial, and industrial consumers, where consumers can choose one of the offered packages and participate in a demand response program depending on their conditions. Rayleigh and beta PDFs are proposed to model the wind and solar power generation. The proposed multi-objective model is solved by using Multi-Objective Particle Swarm Optimization (MOPSO) method, considering the Pareto criterion with nonlinear sorting based on fuzzy mechanism.

In short, the main contributions of this study are:

- The use of DRPs to cover the uncertainty caused by wind and solar power generation in a smart microgrid by considering the objective functions related to the operation costs and pollution emissions.
- Propose the use of offered packages of price strategy in order to implement demand response programs.
- Use probabilistic modeling of wind, solar, and wind-solar powers as a function of output power generation to provide more compliance between planning and reality.
- Consider a probabilistic multi-objective model and use the MOPSO method by considering Pareto criterion and fuzzy-based mechanism to solve the intended problem.

The rest of this paper is organized as follows: after the Introduction, in Section 2, the problem is described in detail. In Section 3, the studied smart micro-grid is introduced. In Section 4, the proposed algorithm is presented based on Pareto criterion. In Section 5, the simulation and analysis of numerical results are discussed, and finally, the last section reports the important conclusions of this study.

2. Statement of the problem

In this study, a probabilistic model is proposed for short-term energy management in order to minimize the operational cost and emissions in a smart micro-grid. Due to the stochastic behavior of wind and solar energies, their accurate prediction is not possible and is always associated with uncertainty error in next-day planning. Therefore, to provide more compliance between planning and reality, a PDF is used to model the behaviors of wind, solar and hybrid solar-wind power systems in an attempt to obtain optimal results despite uncertainties. To remove the uncertainty induced by these resources, incentive-based payment demand response programs are proposed. However, it is assumed that planning for generation resources and consumption demands in a smart micro-grid is performed by the distribution system's operator, which has the possibility of managing and controlling the grid using distribution management systems and advanced metering infrastructure. The following section is dedicated to the modeling and introduction of the objective function.

2.1. Proposed model for Wind Energy System (WES)

Wind turbines convert wind energy into electrical energy. Output power from the wind turbine depends on parameters, such as wind availability, wind speed, the wind turbine's power curve, and shape and size of the turbine. Probabilistic models are developed based on available historical information; since wind speed is a stochastic variable, the meteorological data can be appropriate for

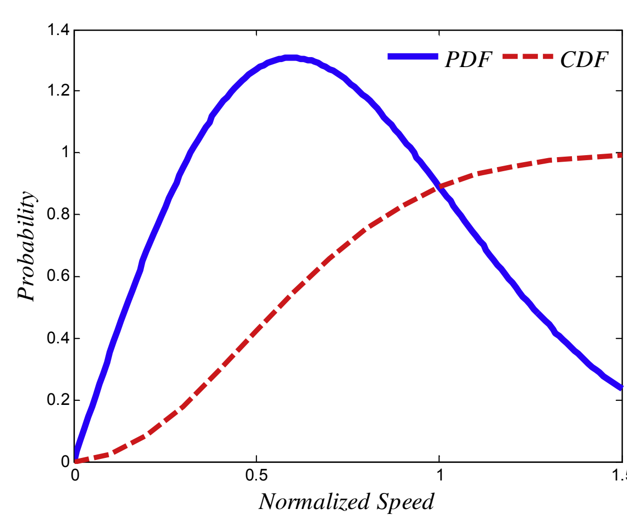

Fig. 1. Wind speed distribution model.

estimating the wind energy potential of a site. According to the wind speed behavior, Rayleigh distribution is used to model wind [18]. Rayleigh distribution is a particular form of Weibull distribution in which the shape index is equal to 2. Therefore, assuming α_w as the scale parameter, and $\beta_w=2$ as the shape parameter, the probability density and cumulative distribution functions are as follows:

$$F_V(v_{wind}) = 1 - \exp\left(-\left(\frac{v_{wind}}{\alpha_w}\right)^2\right) \tag{1}$$

$$f_V(v_{wind}) = \frac{2}{\alpha_w^2} v_{wind} \exp\left(-\left(\frac{v_{wind}}{\alpha_w}\right)^2\right) \tag{2}$$

If v_m is considered the average wind speed of a specific site, the scale parameter is given:

$$\begin{aligned} v_m &= \alpha_w \Gamma\left(1+\frac{1}{2}\right) = \frac{1}{2}\alpha_w \Gamma\left(\frac{1}{2}\right) = \frac{\sqrt{\pi}}{2}\alpha_w \\ \alpha_w &= \frac{2}{\sqrt{\pi}} v_m \end{aligned} \tag{3}$$

Therefore, in the case of substituting α_w in Probability Density Function (PDF) and Cumulative Distribution Function (CDF), the Rayleigh model for Wind Energy System (WES) will be obtained as a function of average wind speed according to (4) and (5). Fig. 1 demonstrates a sample of probability density and cumulative distribution functions.

$$f_V(v_{wind}) = \frac{\pi}{2}\frac{v_{wind}}{v_m^2} \exp\left(-\left(\frac{\pi}{4}\right)\left(\frac{v_{wind}}{v_m}\right)^2\right) \tag{4}$$

$$F_V(v_{wind}) = 1 - \exp\left(-\left(\frac{\pi}{4}\right)\left(\frac{v_{wind}}{v_m}\right)^2\right) \tag{5}$$

For a certain WES, the characteristic of the output power can be defined as below [19]:

$$P_w(v_{wind}) = \begin{cases} 0 & v_{wind} < v_{ci} \\ P_R \dfrac{(v_{wind} - v_{ci})}{(v_r - v_{ci})} & v_{ci} \le v_{wind} < v_r \\ P_R & v_r \le v_{wind} < v_{co} \\ 0 & v_{wind} \ge v_{co} \end{cases} \tag{6}$$

where v_{ci}, v_r, v_{co}, and v_{wind} are the cut-in speed, rated speed, cut-off speed, and actual speed of the wind turbine, respectively, and P_R is the rated power of the turbine. The wind turbine used in this study is of AIR403 type [20], where, $P_R = 15kW; v_{ci} = 3.5m/s; v_{co} = 18m/s; v_r = 17.5m/s$. Fig. 2 shows the power curve for this wind turbine.

In this paper, the PDF $f_{Pw}(P_w)$ for the output power of WES can be obtained using Eqs. (4) and (6) by the application of the transformation theorem [21] as:

2.2. Proposed model for photovoltaic system (PVS)

Photovoltaic generators are systems that convert sunlight into electricity in a way that the solar system output is entirely dependent on the amount of sun radiation. Considering the solar irradiance behavior, beta PDF and CDF are used to model it according to (8) and (9) [22,23].

$$f_B(si) = \begin{cases} \dfrac{\Gamma(\alpha+\beta)}{\Gamma(\alpha)\Gamma(\beta)} si^{\alpha-1}(1-si)^{\beta-1} & 0 \le si \le 1, \alpha \ge 0, \beta \ge 0 \\ 0 & \text{otherwise} \end{cases} \tag{8}$$

$$F_B(si) = \int_0^{si} \frac{\Gamma(\alpha+\beta)}{\Gamma(\alpha)\Gamma(\beta)} si^{\alpha-1}(1-si)^{\beta-1} dsi \tag{9}$$

where *si* indicates the amount of solar irradiance (kW/m^2). α and β are parameters of beta PDF that can be calculated from the mean value and standard deviation of solar irradiance data and are utilized as follows:

$$\alpha = \mu\left(\frac{\mu(1+\mu)}{\sigma^2} - 1\right) \tag{10}$$

$$\beta = (1-\mu)\left(\frac{\mu(1+\mu)}{\sigma^2} - 1\right) \tag{11}$$

Now, solar irradiance can be converted into solar power using Eq. (12) [24].

$$P_{PV}(si) = A_c \cdot \eta \cdot si \tag{12}$$

where $P_{PV}(si)$ indicates the amount of output power from PV (kW) for the amount of irradiance s; A_c is surface areas of the arrays (m^2); and η is efficiency of the PV system.

Therefore, in the case of using Eq. (8), the probability density function $f_B(P_{PV})$ for the output power of PVS is expressed as follows:

$$f_{P_{PV}}(P_{PV}) = \begin{cases} \dfrac{\Gamma(\alpha+\beta)}{\Gamma(\alpha)\Gamma(\beta)} (A_c\eta si)^{\alpha-1}(1-A_c\eta si)^{\beta-1} & \text{if } P_{PV} \in [0, P_{PV}(si)] \\ 0 & \text{otherwise} \end{cases} \tag{13}$$

2.3. Proposed model for hybrid solar-wind power system (HSWPS)

Power generation by hybrid system P_h is equal to total power output from WES system plus the power output from PVS system.

$$P_h = P_w + P_{PV} \tag{14}$$

Assuming that P_W and P_{PV} are independent in terms of performance in accordance with relations (6) and (12), density function

$$f_{P_W}(P_w) = \begin{cases} 1 - [F_v(v_{co}) - F_v(v_{ci})] & P_w = 0 \\ \left(\dfrac{v_r - v_{ci}}{P_R}\right) \cdot \left(\dfrac{\pi}{2v_m^2}\right) \times \left(v_{ci} + (v_r - v_{ci}) \cdot \dfrac{P_w}{P_R}\right) \times \exp\left[-\left(\dfrac{v_{ci} + (v_r - v_c)\frac{P_w}{P_R}}{\frac{2}{\sqrt{\pi}} v_m}\right)^2\right] & 0 < P_w < P_R \\ F_v(v_{co}) - F_v(v_r) & P_w = P_R \end{cases} \tag{7}$$

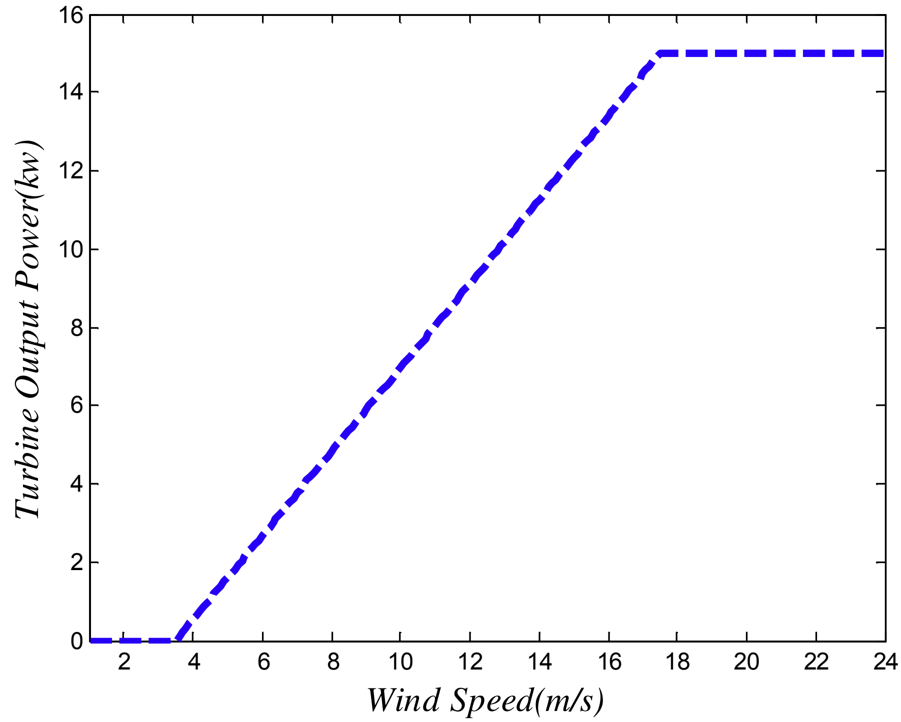

Fig. 2. Wind turbine model AIR403 power curve.

for random variable P_h as convolution between density functions P_W and P_{PV} is defined as follows [25]:

$$f_h(P_h) = f_{P_W}(P_W) * f_{P_{PV}}(P_{PV}) \tag{15}$$

Since representing the continuous PDF in the mathematical form seems to be difficult, the application of Monte Carlo simulation is used in such cases to achieve different scenarios; yet, generating different scenarios also adds to the mathematical complexities of the problem. The appropriate strategy for preventing mathematical complexities is to discretize the continuous PDF by dividing it into different intervals. Depending on the desired accuracy, PDF function can be divided into a number of discrete instants with different possible levels. In this case, the surface enclosed by each interval represents the median probability of that interval. Therefore, in this paper, the probability density function proposed for each wind and solar system is divided into seven ranges per hour in order to supply the requested power. As a result, any wind and solar systems have seven scenarios to participate in production planning every hour.

2.4. Model of demand response programs

In the present study, electricity consumers are considered to be residential, commercial, and industrial, and the following equations demonstrate the modeling for their behavior. Constraints show that sum of energy reduction by each consumer at every hour should be lower or equal to the maximum amount of its offers.

$$RP(r,t) = RC(r,t) \cdot \zeta_{r,t} \quad , RC(r,t) \le RC_t^{max} \tag{16}$$

$$CP(c,t) = CC(c,t) \cdot \zeta_{c,t} \quad , CC(c,t) \le CC_t^{max} \tag{17}$$

$$IP(i,t) = IC(i,t) \cdot \zeta_{i,t} \quad , IC(i,t) \le IC_t^{max} \tag{18}$$

where *r*, *c*, and *i* represent the number of residential, commercial, and industrial consumers; *RC*(*r*,*t*), *CC*(*c*,*t*), and *IC*(*i*,*t*) indicate the amount of load reduction planned by each residential, commercial, and industrial consumer in period *t*; RC_t^{max}, CC_t^{max}, and IC_t^{max} indicate the maximum load reduction proposed by each consumer in period *t*; $\zeta_{r,t}$, $\zeta_{c,t}$, and $\zeta_{i,t}$ show the amount of incentive payment

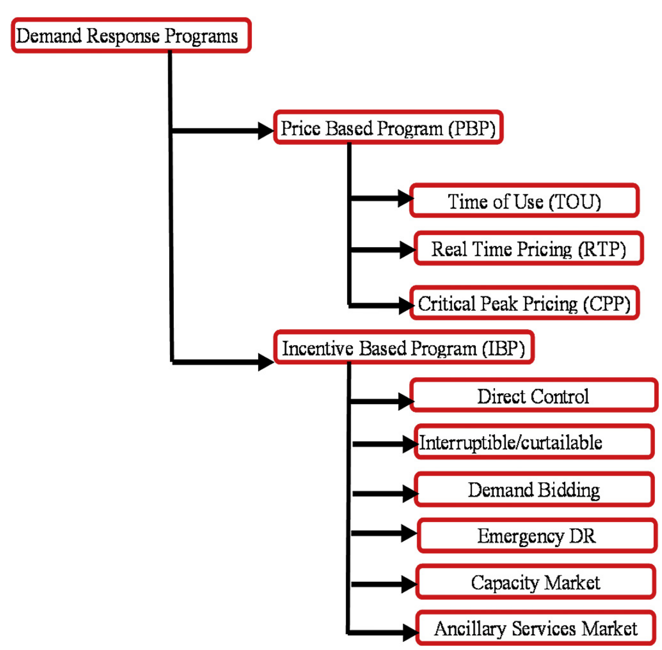

Fig. 3. Classification of DRPs.

to each consumer in period t; and $RP(r,t)$, $CP(c,t)$, and $IP(i,t)$ represent the cost due to load reduction by residential, commercial, and industrial consumers in period t for the proposed load reduction, respectively.

2.5. Objective functions

Demand response can be categorized based on the consumer's participation in changing their consumption behavior into two groups of price-based and incentive-based demand response programs (Fig. 3), and each of these groups is divided into several subgroups. More detail is presented in Refs. [9,10].

Since incentive-based responsibility programs deal with price signals and are considered voluntary, modeling it on the basis of offering packages of price, given the reduced amount of demand, is represented as Fig. 4 by considering the demand response programs based on incentive payment.

$$\mathrm{COC(t)} = \sum_{i=1}^{N_{DG}} \left[P_i(t)\pi_i(t)I_i(t) + SU_i(t)|I_i(t) - I_i(t-1)| + RC_i^{DG}(t)\right] + \sum_{j=1}^{J} RC_j^{DR}(t) I_{Buy}(t) P_{Grid-Buy}(t)\pi_{Grid-Buy}(t) - I_{Sell}(t)P_{Grid-Sell}(t)\pi_{Grid-Sell}(t) \tag{20}$$

In this study, a multi-objective stochastic programming model will consider operation costs and pollution emissions in the presence of distributed generation resources and wind and solar sources. Moreover, DRPs based on incentive-based payment will be used to remove the uncertainty caused by the random behavior of wind and solar resources in a 24-h planning period. In these programs, demands are considered as responsive residential, commercial, and industrial demand. Fig. 5 shows a clear picture of the optimization model.

2.5.1. Operational cost function

Here, the operation function is divided into two parts: certain operational costs - including the fixed running and start-up costs of Distribution Generations (DGs), spinning and non-spinning reserve costs provided by DGs, as well as demand response programs - and costs of power, which is bought/sold from/to the utility; and uncertain operational costs - by considering and realizing the probability of scenario Pr_s during the t th period and sth scenario, which are affected by the probabilistic amounts of wind and solar parameters in each scenario. This part of the operational cost function includes the running cost of distributed generation units, cost of load reduction due to demand response programs, and costs associated with Value of Lost Load (VOLL) and Expected Energy Not Served (EENS) for consumers.

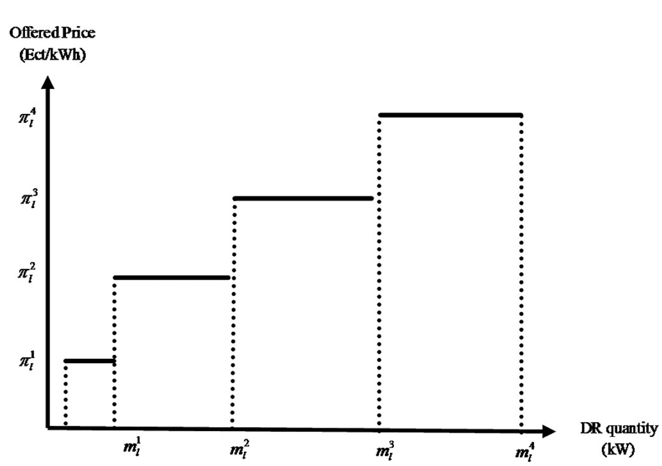

Fig. 4. DRP's offer package.

$$\mathrm{Min}\ f_1(X) = \sum_{t=1}^{T} F^{Cost}(t) = \sum_{t=1}^{T} \mathrm{COC}(t) + \sum_{t=1}^{T}\sum_{s=1}^{S} Pr_s \times UOC_s(t) \tag{19}$$

where Pr_s is the probability of scenario s. Certain and uncertain operational cost functions are defined according to (20) and (21), respectively.

$$\mathrm{UOC_s(t)} = \sum_{i=1}^{N_{DG}} C_{i,s}^{DG}(t) + \sum_{j=1}^{J} C_{j,s}^{DR}(t) + ENS_s(t) \times VOLL(t) \tag{21}$$

where $P_i(t)$ and $\pi_i(t)$ indicate the amount of output power and offered price for the ith unit during the t th period; binary $I_i(t)$ represents the on and off mode of the ith DG during the t th period; $SU_i(t)$ shows running and shutting down costs for the ith unit during the t th period; $RC_i^{DG}(t)$ and $RC_j^{DR}(t)$ are reserve costs of the ith DG and demand response programs for the j th load during the t th period; $P_{Grid\text{-}Buy}(t)$ and $P_{Grid\text{-}sell}(t)$ represent the amount of exchange power with utility in period t; $\pi_{Grid\text{-}Buy}(t)$ and $\pi_{Grid\text{-}sell}(t)$ indicate the offered price for exchange power with utility in the open electricity market during the t th period; $C_{i,s}^{DG}(t)$ and $C_{j,s}^{DR}(t)$ show the running cost of the ith DG unit and the cost due to load reduction provided by the j th DRPs during the t th period in the sth scenario; and $ENS_s(t)$ and $VOLL(t)$ are the Expected Energy Not Served (EENS) in the sth scenario at t th period and Value of Lost Load (VOLL) at t th period, respectively. In Eq. (19), $X^T = [X_1, X_2, \ldots, X_T]$ is the variables state vector that includes active power produced by each DG, charge and discharge power of the battery, and the active power exchanging with the upstream grid.

Regarding the operational costs in the proposed model, it is assumed that DGs, along with the DRs, are the spinning reserve providers for compensating the uncertainty caused by wind and solar, renewable generations. Therefore, the DG that is considered in the off mode at its ground state is turned on to provide reserve power; thus, fixed and start-up costs of DGs with the possibility equal to unity are included in the first part of the operational cost function. In other words, during the occurrence of scenario in on/off real-time modes, the DG remained constant during the planning, and output power was only carried out according to the programmed values for the day ahead. Hence, in the real-time occurrence of each scenario, the reverse payment would not change and, as a result, the reserve cost is considered with the possibility of one in the first parts of the objective function.

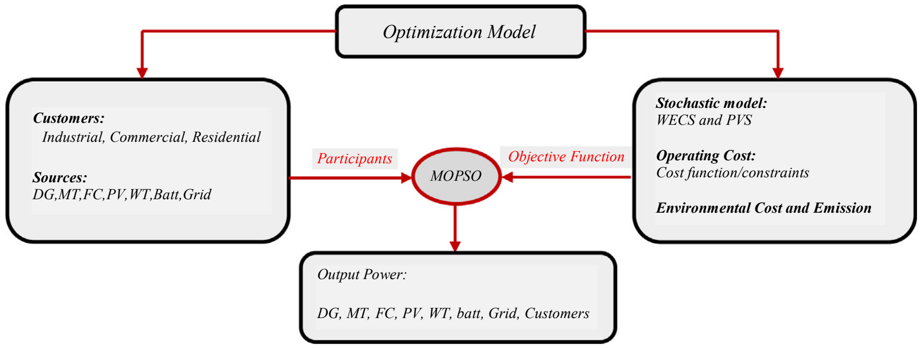

Fig. 5. Optimization model structure.

2.5.2. Pollution emissions function

Pollution emissions function includes functions such as the amount of pollution caused by DG units and the amount of pollution caused by the grid at the time of purchase. The pollutants include CO_2, SO_2, and NO_x, and the mathematical model of pollution emissions function can be obtained as follows:

$$\text{Min } f_2(X) = \sum_{t=1}^{T} F^{\text{Emission}}(t) = \sum_{t=1}^{T} \left[\text{Emi}_{DG}(t) + \text{Emi}_{Grid}(t)\right] \tag{22}$$

The average pollution caused by renewable DG units can be calculated as follows:

$$\text{Emi}_{DG}(t) = \sum_{i=1}^{N_{DG}} \left(E_{CO_2}^{DG}(i) + E_{SO_2}^{DG}(i) + E_{NO_x}^{DG}(t)\right) \times P_i^{DG}(t) \tag{23}$$

where $E_{CO_2}^{DG}(i)$, $E_{SO_2}^{DG}(i)$, and $E_{NO_x}^{DG}(i)$ indicate the amount of CO_2, SO_2, and NO_x, pollution caused by the ith DG, respectively, that kg/MWh is its measurement unit. Similarly, pollution caused by the grid at the time of energy purchase can be written as follows:

$$\text{Emi}_{Grid}(t) = \left(E_{CO_2}^{Grid} + E_{SO_2}^{Grid} + E_{NO_x}^{Grid}\right) \times P_{Grid}(t) \tag{24}$$

2.6. Problem constraints

The typical smart microgrid is assumed to operate with the following constraints.

2.6.1. Power balance constraint

The total power generated by DGs purchased from the utility; and load reduction caused by demand response programs in each interval and scenario must be equal to the total demand loads.

$$\sum_{i=1}^{N_{DG}} P_{DG,i,s}(t) + P_{Grid,s}(t) = \sum_{l=1}^{N_s} P_{Demand_{l,s}}(t) - P_{DR,s}(t) \tag{25}$$

where $P_{Demand\ l,s}$ is the amount of L th demand level during the t th period and sth scenario. In Eq. (26), $P_{DR,s}(t)$ is the amount of active power participation in demand response programs and can be described as follows:

$$P_{DR,s}(t) = \sum_{r} RC(r,t,s) + \sum_{c} CC(c,t,s) + \sum_{i} IC(i,t,s) \tag{26}$$

2.6.2. Reserve and DG power constraint

Maximum and minimum power generations by each unit are constrained and can be expressed as follows:

$$P_{DG,i}^{min}.I(i,t) \le P_{DG}(i,t,s) \le P_{DG,i}^{max}\cdot I(i,t) \quad \forall i,t,s \tag{27}$$

$$R_{DG}(i,t) \ge P_{DG}(i,t,s) - P_{DG}(i,t,0) \quad \forall\ i,t,s \tag{28}$$

2.6.3. Battery constraints

Since there are limitations of charging and discharging in storage devices during each time interval, the following limitations and equations can be expressed for a battery type:

$$\begin{aligned} W_{ess}(t) &= W_{ess}(t-1) + \eta_{charge}(t)P_{charge}(t)\Delta t\cdot I_{charge} \\ &\quad - \frac{1}{\eta_{discharge}}P_{discharge}(t)\Delta t\cdot I_{discharge}I_{discharge}(t) + I_{charge}(t) \\ &\quad \le 1W_{ess,min} \le W_{ess}(t) \le W_{ess,max}P_{charge}(t) \\ &\quad \le P_{charge,max};\ \ P_{discharge}(t) \le P_{discharge,max} \end{aligned} \tag{29}$$

where, $W_{ess}(t)$ and W_{ess} (t-1) separately; shows the amount of energy stored within the battery at t and t-1 time; P_{charge} ($P_{discharge}$) is the amount of allowed charge/discharge during a defined period of time (Δt), η_{charge} ($\eta_{discharge}$) is battery efficiency during charging/discharging; $W_{ess,min}$ and $W_{ess,max}$ are lowest and the highest amounts of energy stored in the battery; and $P_{chrge,max}$ ($P_{discharge,max}$) is maximum battery charge/discharge during each time interval Δt.

2.7. Typical smart microgrid system

A microgrid usually includes a set of DGs, energy reserves, and load systems that can be operated independently or in conjunction with the area's main electrical grid [26,27]. Development of micro-grids is a part of a smart grid concept; due to the advantages of micro-grids, such as reduced energy costs and improved reliability and system security, it is obvious that there are common objectives among micro-grids and smart grids [28]. Also, advantages such as green technology development and the use of demand response programs in micro-grids depend on the use of smart grid technologies. As observed in Fig. 6, the smart micro-grid studied here has three types of consumers: residential, commercial, and industrial, along with power generation resources such as Micro-Turbine (MT), Wind Turbine (WT), Photovoltaic (PV) cell, Fuel Cell (FC), and battery and diesel generators; therefore, this grid has the capacity to exchange energy with the utility. The installation characteristics

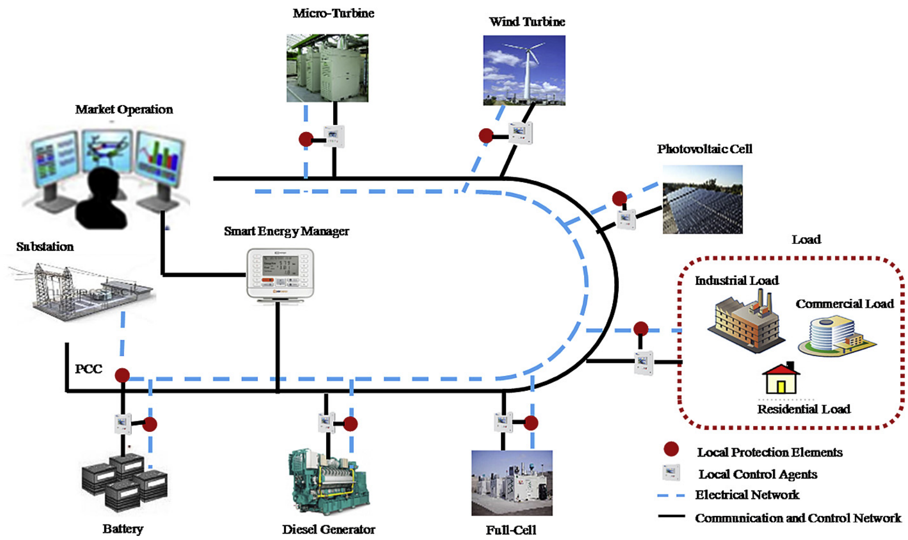

Fig. 6. Typical smart micro-grid system.

Table 1
Bids and emissions coefficient of the DG sources.

Unit	Type	Bid (€ct/kWh)	Start-up/Shut-down Cost (€ct)	CO_2 (kg/MWh)	SO_2 (kg/MWh)	NO_x (kg/MWh)	$P_{\min}(kW)$	$P_{\max}(kW)$
1	Diesel	0.586	0.15	890	0.0045	0.23	30	300
2	MT	0.457	0.96	720	0.0036	0.1	6	30
3	FC	0.294	1.65	460	0.003	0.0075	3	30
4	PV	2.584	0	0	0	0	0	25
5	WT	1.073	0	0	0	0	0	15
6	Bat	0.38	0	10	0.0002	0.001	−30	30
7	Grid	–	0	950	0.5	2.1	−30	30

are presented in Table 1, which includes DG price offers, cost of starting up and shutting down of units, amount of greenhouse gas emissions caused by DGs and utility, as well as minimum and maximum power generations [29].

3. MOPSO algorithm

Since multi-objective optimization problems include multiple conflicting objective functions, equality constraints and inequalities must be optimized simultaneously.

$$\begin{aligned} &Min\ \ F(X) = [f_1(X) \quad f_2(X) \quad \ldots \quad f_n(X)]^T \\ &Subject\ \ to: \begin{cases} g_i(X) < 0 & i = 1, 2, \ldots, N_{ueq} \\ h_i(X) = 0 & i = 1, 2, \ldots, N_{eq} \end{cases} \end{aligned} \tag{30}$$

where F(X) is a vector containing objective functions and X is a vector containing optimization variables, $f_i(X)$ is the objective function *i*th; $g_i(X)$ and $h_i(X)$ are constraints of equality and inequality; and n is the number of objective functions. For a multi-objective optimization problem either X or Y solutions can be one of the two possible solutions. One will dominate another, or none is dominated by any of the other solutions. Therefore, in an optimization problem, one solution X will dominate Y if the following two conditions are met:

$$\begin{aligned} &\forall\ \ j \in \{1, 2, \ldots, n\}, \quad f_j(X) \le f_j(Y) \\ &\exists\ \ k \in \{1, 2, \ldots, n\}, \quad f_k(X) < f_k(Y) \end{aligned} \tag{31}$$

Therefore, the Pareto set solutions can be obtained through non-dominated solutions (desired answers) on search space. Finally, the answer is obtained among non-dominated solutions stored in the archive.

In this study, the concept of Pareto optimization is applied to the basic principles of PSO algorithm [30] (developing the algorithm of Multi-Objective Particle Swarm Optimization (MOPSO) [31]), simultaneous minimization of operational costs and emission functions with renewable generation, and DG and DR which are carried out. Application of the algorithm to the problem considered in this study can be accomplished with the following steps.

Step 1: Defining the input data.

These data are related to smart micro-grid technical specifications and include production capacity, proposed power price, and the operational and emission costs of DGs. In addition, the data include the mean values and variance of wind speed and solar irradiance on the next day, and the requested demand from the daily load curve.

Step 2: Obtaining the amount of wind and solar power from proposed equations.

Step 3: Generating an initial population as $X^T = [X_1, X_2, \ldots, X_T]$.

Step 4: Applying a power dispatch algorithm to the generated population and calculation of fitness function according to Eq. (19) or (22).

Step 5: Identifying non-dominated solutions.

Step 6: Separating non-dominated solutions and storing them in an archive.

Step 7: Selecting the best particle from the non-dominated response archive as a leader.

The process of selecting a leader is as follows:

The explored search space is divided into equal parts and a probability distribution is distributed to each part. Finally, the best particle is selected as the leader using the roulette wheel method.

Step 8: Updating the new velocity and position for each particle.

Step 9: Updating the best position for each particle.

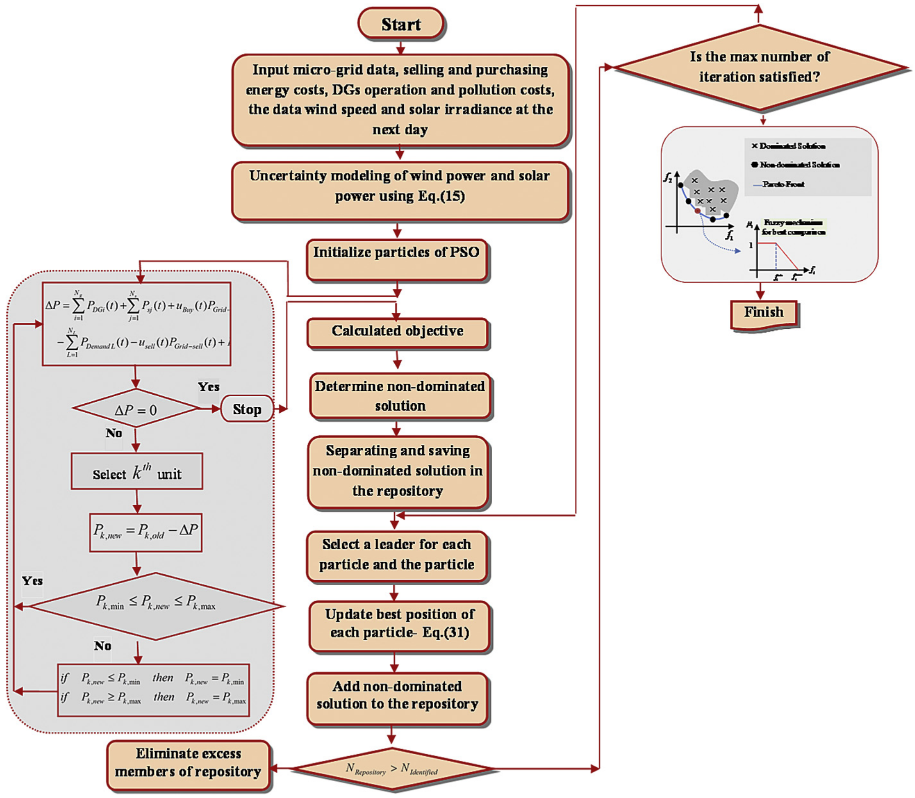

Fig. 7. Flowchart of MOPSO algorithm.

For updating the best position, the particle's new position is compared with its previous position.

$$P_{best,i}(t+1) = \begin{cases} P_{best,i}(t) & P_{best,i}(t) \prec X_i(t+1) \\ X_i(t+1) & X_i(t+1) \prec P_{best,i}(t) \\ \text{select randomly} & \\ (P_{best,i}(t) \text{or} X_i(t+1)) & \text{otherwise} \end{cases} \quad (32)$$

Step 10: Adding the current non-dominated solutions to the archive.

Step 11: Removing the dominated solutions from the archive.

Step 12: If the number of members in the archive exceeds the determined capacity, extra members would be removed.

Step 13: Evaluating the criterion for program termination.

If the maximum number of repetitions is established, the optimization process would stop; otherwise, the current population would replace the previous population, and the algorithm would return to Step 7.

Step 14: Selecting the best interactive solution.

In order to choose a better solution from among the obtained optimal responses, the fuzzy decision-making function with a membership function is considered, in which the exact number of variables can be located; where μ_i^k represents the optimality amount of the objective function i in among Pareto optimal response k, which is calculated as follows:

$$\mu_i^k = \begin{cases} 1 & f_i \le f_i^{\min} \\ \dfrac{f_i^{\max} - f_i}{f_i^{\max} - f_i^{\min}} & f_i^{\max} < f_i < f_i^{\min} \\ 0 & f_i \ge f_i^{\max} \end{cases} \quad (33)$$

where $f_i^{\max}$ and $f_i^{\min}$ are the upper and lower limits of the objective function i, respectively. In the proposed method, these values are calculated using optimization results for each objective function. μ_i^k is in the range of 0–1 such that $\mu_i^k = 0$ indicates incompatibility of the solution with the objectives of designer, while $\mu_i^k = 1$ represents full compatibility.

Fig. 7 shows the flowchart of the proposed algorithm used for solving the optimization problem.

4. Simulation and analysis of numerical results

The smart microgrid connected to the utility in Fig. 6 has three residential, commercial, and industrial consumers whose load demand from the system and daily load curve are shown in Fig. 8 [32]. It is considered a test system, so that the total energy consumption during the day is equal to 4034 *kWh*. The real-time market price of APX is shown in Fig. 9 [33].

The spinning reserve cost due to DGs is considered to be 20% of the highest marginal cost of energy generation [34]. Hourly wind speed data, which are taken from the weather forecast website (Willy Online Ply Ltd.) [35], are shown in Fig. 10. The solar cell considered here is a 25 kW SOLAREX MSX, composed of solar panels of *10×2.5 kW* with η=*18.6%* and s=*10m*^{2} [36]; Fig. 11 shows the average hourly solar irradiance [37].

It is assumed that the power coefficient of the wind turbine and PV system is equal to 1, while other DGs and loads locally compensate for the required reactive power through capacitor placement in the related buses. The value of lost load is considered to be equal to *1.33 €/kWh* [38]. In a typical system, including a battery with a capacity of *30kWh*, minimum and maximum charges are considered to be 10% and 100% of the battery capacity, respectively, with a charge and discharge efficiency of 94% [39,40]. The offered packages provided for demand response programs are shown in Table 2. For their implementation, it is assumed that 40% of consumers participate in demand response programs [41].

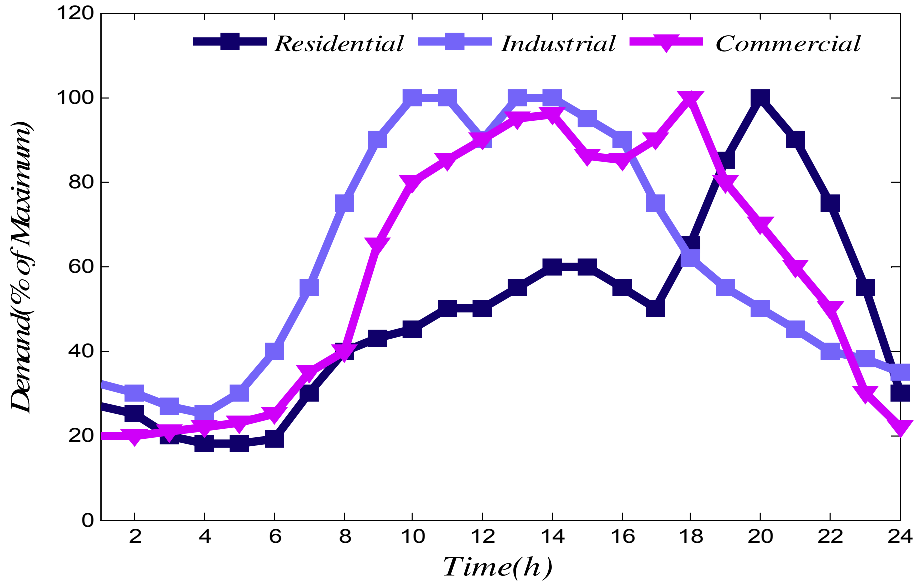

Fig. 8. Daily load curves for different consumers.

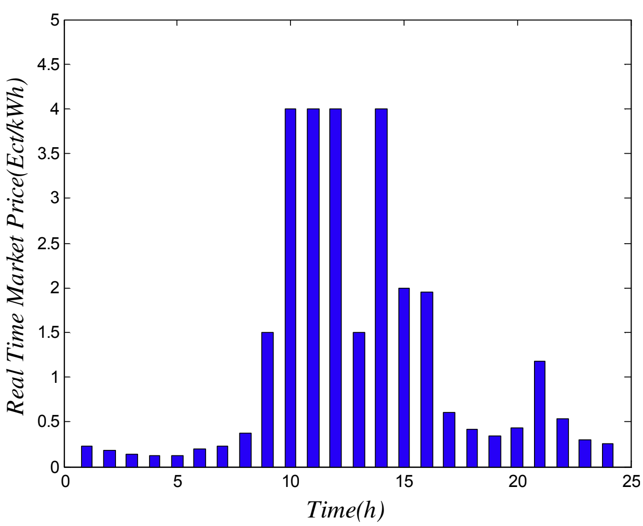

Fig. 9. The real-time market prices of APX.

To evaluate the effect of planning for energy level, reserve, and DR in the operational costs and pollution emissions function, and to resolve the uncertainty caused by wind and solar resources, the problem is considered in three different conditions:

- Case 1: Considering operational cost and emission functions without demand response
- Case 2: Considering operational cost and emission functions with demand response
- Case 3: Simultaneously considering multi-objective functions of operational costs and emissions

In all the cases, power generation units are supposed to have the capability of participating in the smart microgrid depending on their technical and economic characteristics and exchange of energy with the utility through a Point of Common Coupling (PCC) in the case of excessive generation and demand. In order to evaluate the effects of the proposed model, it has been implemented in MATLAB software on a PC (2.6 MHz with 4 GB of RAM).

Case 1: *Operational cost and emission functions without demand response*

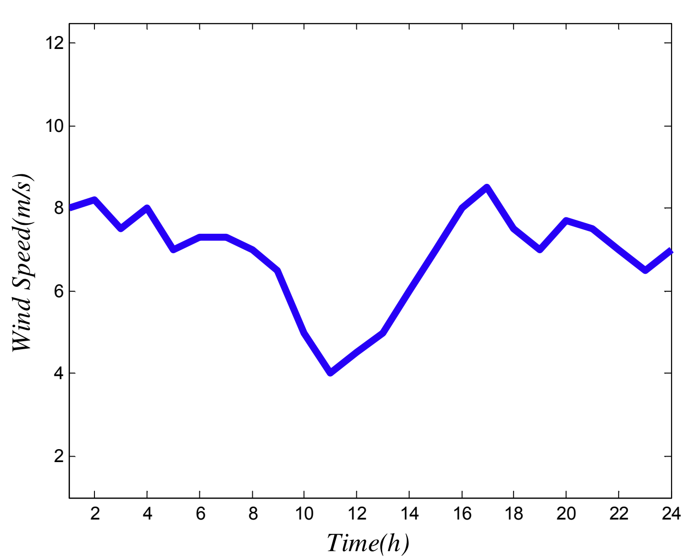

Fig. 10. Hourly wind speed forecast.

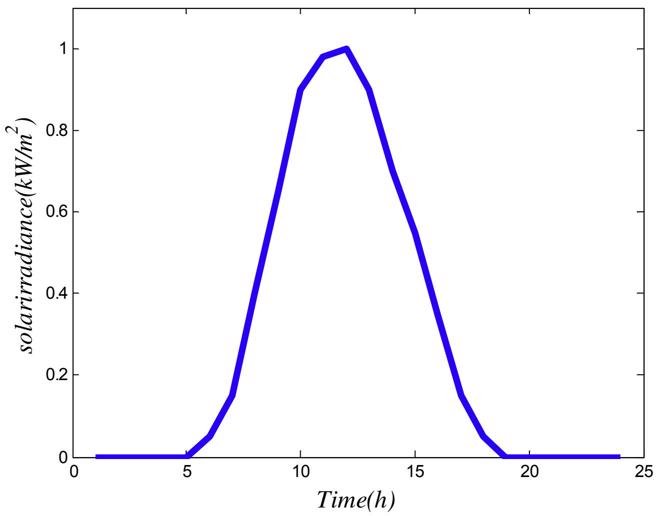

Fig. 11. Hourly solar irradiance forecast.

Table 2
Price-quantity offer package for DRPs.

Quantity (kW)				
Price (€ct/kWh)				
DRP_1	0–5	5–10	10–50	50–70
	0.06	0.13	0.26	0.36
DRP_2	0–5	5–20	20–30	30–60
	0.04	0.07	0.28	0.43

In this case, the operational costs and emission are separately minimized without considering the DR. The optimal allocation of the power generation of the units for minimizing the operational costs and emissions is shown in Tables 3 and 4, respectively. The results of Table 3 suggest that in the early hours, when the price of energy is low, the battery starts to be charged, and from 9 to 16, when energy prices are high, the utility purchases energy from the smart microgrid in which the power consumption is provided by DGs with the priority of offered price. The results of Table 4 show that, in most operational periods, due to the high pollution of utility, the utility purchases power from the smart microgrid in most of the periods. Results in Fig. 12 indicate that, since wind and solar power are devoid of any pollution most of the time, these resources reach their maximum power generation by considering the pollution emission function.

However, since the offered price of these resources is higher than that of other power generation resources, they cannot receive much attention when considering the optimal operational cost. Results reported in Ref. [29] verify this conclusion.

Case 2: *Operational cost and emissions functions with demand response*

In this step, operational costs and emissions are separately minimized with the involvement of DR. The optimal allocation of power generation of units for minimizing operational costs and emissions is shown in Tables 5 and 6, respectively.

Comparison of the results presented in Tables 3 and 5 show that, in the case of using demand response programs, wind power generation is reduced from *8.51 kW* to *7.87 kW*, and solar power generation is reduced from *4.82 kW* to *3.34 kW*. On the other hand, comparison of results obtained from the optimization of emission function with/without DR indicates that use of these programs reduces the wind and solar power generations from *50.61 kW* to *47.39 kW*, and from *91.39 kW* to *89.50 kW*, respectively. Fig. 13 shows the amount of power generation by wind turbine and solar cell considering the operational cost and pollution emissions with the involvement of demand response.

According to Fig. 14, it can be said that, considering the pollution emissions, the use of DRPs reduces the production capacity of wind turbine and solar cell, and also shifts the demand from peak periods to off-peak periods. In this case, when the customers participate in the DR program and accept a reduction of their consumption at a specific hour, it allows the system operator to reduce the scheduled power of generating units.

Case 3: *Simultaneous consideration of multi-objective operational*

Table 3
Energy resources scheduling for operation cost objective function without DR.

Hour	units						
	DG (kW)	MT (kW)	FC(kW)	WT (kW)	PV(kW)	Batt (kW)	Utility (kW)
1	30.000	7.9514	7.283	0.178	0.000	11.587	30.000
2	32.287	12.912	27.010	0.178	0.000	−19.688	26.299
3	45.130	7.189	20.433	0.069	0.000	−19.786	21.963
4	38.075	6.000	24.565	0.000	0.000	−30.000	29.359
5	30.000	8.835	13.957	0.403	0.000	−14.207	26.011
6	37.393	8.068	23.610	0.091	0.000	−21.981	23.818
7	30.000	12.489	19.287	0.016	0.000	−0.705	22.912
8	33.650	9.813	26.953	0.063	0.075	26.505	22.939
9	104.789	28.719	21.201	0.178	0.112	30.000	−30.000
10	234.763	6.000	3.213	0.000	0.000	−15.975	−30.000
11	211.313	8.245	19.145	0.000	0.851	15.444	−30.000
12	283.868	6.000	5.132	0.000	0.000	−30.000	−30.000
13	272.073	6.000	8.400	0.054	1.695	−28.255	−29.966
14	218.992	13.747	24.529	0.473	0.342	21.758	−29.843
15	213.897	14.123	28.932	0.714	0.859	27.265	−29.791
16	226.268	13.190	6.804	0.300	0.338	24.099	−30.000
17	114.225	29.999	29.974	0.000	0.550	30.000	25.252
18	95.459	27.799	30.000	1.741	0.000	30.000	30.000
19	105.819	29.999	30.000	1.302	0.000	30.000	29.879
20	122.196	14.555	29.017	0.000	0.000	26.876	27.355
21	155.728	28.322	28.442	1.300	0.000	30.000	−23.792
22	79.629	28.946	26.685	0.555	0.000	29.860	29.323
23	54.699	29.097	25.325	0.717	0.000	25.161	30.000
24	31.509	10.515	26.946	0.172	0.000	28.682	25.174

Table 4
Energy resources scheduling for emission objective function without DR.

Hour	units						
	DG (kW)	MT (kW)	FC(kW)	WT (kW)	PV(kW)	Batt (kW)	Utility (kW)
1	37.654	17.999	29.918	1.428	0.000	30.000	−30.000
2	30.000	23.862	24.679	0.426	0.000	27.435	−27.403
3	30.000	13.837	26.968	1.428	0.000	30.000	−27.233
4	30.105	6.678	30.000	0.801	0.000	30.000	−29.584
5	30.000	6.000	27.317	1.785	0.000	29.897	−30.000
6	30.000	8.457	30.000	0.4146	0.000	30.000	−27.871
7	32.727	16.279	30.000	1.501	0.000	30.000	−26.508
8	50.717	30.000	29.678	1.305	0.197	29.731	−21.628
9	59.526	30.000	30.000	1.630	3.727	30.000	0.116
10	111.604	29.726	28.456	1.809	7.525	29.507	−10.627
11	125.775	30.000	30.000	8.775	10.449	29.999	−20.000
12	152.640	30.000	29.999	10.410	11.950	29.999	−30.000
13	142.210	30.000	29.988	3.915	23.899	29.984	−29.997
14	164.908	30.000	30.000	2.345	21.050	30.000	−28.304
15	175.367	30.000	30.000	1.780	7.875	30.000	−19.027
16	161.097	29.987	29.019	1.284	4.225	30.000	−14.607
17	158.091	29.869	27.953	1.593	0.493	30.000	−18.000
18	153.215	30.000	30.000	1.785	0.000	30.000	−30.000
19	115.726	30.000	28.812	1.275	0.000	30.000	21.187
20	108.116	29.540	29.986	1.785	0.000	29.469	21.103
21	98.827	30.000	30.000	1.300	0.000	29.873	30.000
22	73.699	30.000	30.000	1.300	0.000	30.000	29.999
23	44.515	29.573	29.999	0.915	0.000	30.000	29.997
24	38.253	29.227	30.000	0.615	0.000	30.000	−5.096

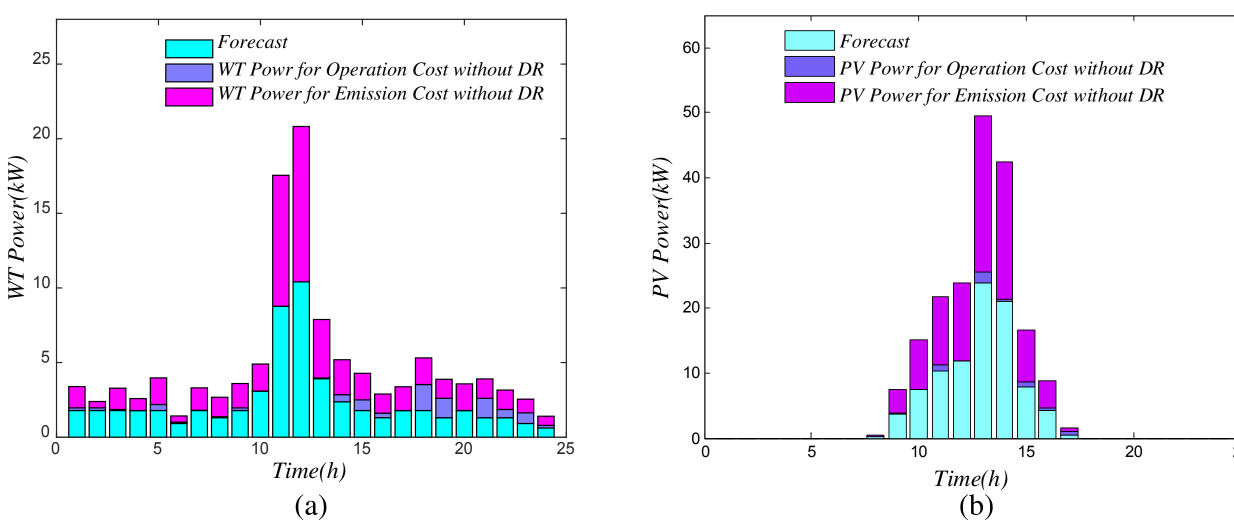

Fig. 12. Output power (a) Wind turbine (b) Solar cell, considering operating cost and emission without DR.

and emission cost functions

In case 3, the optimal power allocation of the units is carried out for the simultaneous minimization of operational costs and emissions as two inconsistent functions with/without the involvement of DR. According to Fig. 15, since the objectives of operational cost and emissions costs are opposite, moving from initial points on curves toward the endpoints along the Pareto path is equal to the change in the operation behavior from low cost and more pollution to higher cost and low pollution, where the optimal operation point can be determined by fuzzy mechanisms.

The results of Fig. 15 indicate that, in the case of using demand response programs, it is possible to improve the optimal operation point such that the operational cost and pollution emissions are reduced by 21% and 14%, respectively. Fig. 16 shows the amount of wind and solar power generation with the minimization of operational cost function and emissions function, as well as with the simultaneous minimization of these two functions when demand response programs are implemented.

The results of Fig. 16 show that maximum wind and solar power generation is related to the case in which pollution emission is taken into account; therefore, it is possible to establish a balance between them by simultaneous optimization.

Results are shown in Table 7 for a better comparison of output wind power and solar cell power from the perspective of operation costs and emissions with/without the presence of demand responses. Results show that among the proposed scenarios, the state of considering the operation cost is the best state to resolve the uncertainty resulted from solar and wind resources.

By comparing the results of simulations calculation of requested power in different cases and the amount of requested energy (4034 kWh), it can be observed that the amount of energy not supplied is negligible and does not have much impact on the results.

Table 5
Energy resources scheduling for operation cost objective function with DR.

Hour	units						
	DG (kW)	MT (kW)	FC(kW)	WT (kW)	PV(kW)	Batt (kW)	Utility (kW)
1	37.694	12.202	8.359	0.243	0.000	0.473	23.029
2	36.791	12.318	13.077	0.000	0.000	−16.677	23.490
3	32.129	15.173	13.239	0.283	0.000	−19.486	23.662
4	31.252	9.991	21.058	0.178	0.000	−29.479	30.000
5	30.178	7.711	3.304	0.000	0.000	−29.998	3.804
6	32.588	6.000	7.898	0.046	0.000	−3.391	17.859
7	36.320	7.426	25.822	0.459	0.000	−20.765	29.736
8	37.811	13.354	29.065	0.030	0.003	26.825	7.911
9	82.384	10.887	22.688	0.178	0.931	27.931	−30.000
10	163.871	22.707	17.409	0.000	0.672	18.340	−30.000
11	239.305	6.475	5.723	0.000	0.000	−1.503	−30.000
12	205.704	8.094	15.044	0.048	0.377	−4.268	−29.999
13	223.543	6.000	27.248	0.005	0.279	−7.202	−29.875
14	267.051	6.000	5.700	0.000	0.000	−3.751	−30.000
15	217.144	25.307	27.230	0.000	0.000	11.251	−29.932
16	175.002	12.794	26.700	0.131	0.531	5.823	−29.981
17	128.741	27.860	29.831	1.785	0.550	29.066	7.166
18	47.588	30.000	29.854	0.000	0.000	27.804	29.753
19	55.726	29.981	30.000	1.302	0.000	29.990	30.000
20	91.621	29.253	28.888	1.747	0.000	28.817	29.674
21	131.616	25.949	24.737	0.769	0.000	26.608	−29.679
22	101.889	16.946	19.488	0.238	0.000	25.349	26.089
23	30.000	14.163	27.543	0.183	0.000	23.249	29.862
24	31.719	15.337	30.000	0.246	0.000	−22.667	28.365

Table 6
Energy resources scheduling for emission objective function with DR.

Hour	units						
	DG (kW)	MT (kW)	FC(kW)	WT (kW)	PV(kW)	Batt (kW)	Utility (kW)
1	30.000	6.000	11.962	0.178	0.000	28.859	−30.000
2	30.704	10.370	25.188	0.107	0.000	29.056	−26.425
3	30.000	11.401	27.743	0.000	0.000	30.000	−29.143
4	30.000	6.000	3.000	0.000	0.000	19.000	−30.000
5	30.000	6.000	3.000	8.58E-19	0.000	6.000	−30.000
6	30.013	6.010	3.051	0.005	0.000	21.862	−29.941
7	32.110	9.840	29.792	1.205	0.000	30.000	−28.956
8	30.000	10.442	23.967	0.000	0.161	30.000	−24.570
9	35.074	30.000	29.692	1.606	3.249	30.000	15.378
10	39.394	29.719	28.609	3.037	7.525	29.878	19.836
11	80.775	30.000	30.000	8.775	10.450	30.000	30.000
12	106.976	29.999	29.791	10.409	11.335	29.994	11.493
13	42.214	30.000	29.986	3.915	23.900	29.999	29.985
14	129.915	29.997	30.000	2.199	21.050	29.969	1.868
15	126.938	29.918	30.000	1.781	7.127	29.991	20.243
16	71.943	30.000	30.000	1.276	4.158	28.990	24.633
17	57.665	30.000	29.999	1.785	0.550	29.999	30.000
18	67.661	30.000	30.000	1.649	0.000	30.000	5.689
19	102.590	30.000	30.000	1.221	0.000	30.000	23.188
20	96.809	30.000	29.999	1.770	0.000	29.582	−18.161
21	58.733	29.999	30.000	1.294	0.000	30.000	29.974
22	36.309	30.000	30.000	1.300	0.000	30.000	17.390
23	51.233	29.999	29.998	0.757	0.000	30.000	18.013
24	33.639	30.000	30.000	0.123	0.000	29.578	−10.341

Results are given in Table 7 for a better comparison of solar and wind generation capacities from the perspective of operating costs and emissions with/without DR. We see that among the proposed modes, taking into account operating costs is the best case to resolve the uncertainty derived from wind and solar resources.

5. Conclusion

In this study, a probabilistic programming was implemented for the smart microgrid, by considering the DR as the compensation for uncertainty caused by wind and solar power generation in the form of an optimization function with two inconsistent objectives. The total operational cost of the microgrid, and pollution caused by pollutants were considered in three different conditions. Moreover, a probabilistic programming method was used to model the stochastic behavior of the wind and solar cells' power generation. For better performance of the smart microgrid, the possibility of energy exchange with the utility was assumed.

In order to manage consumption, it is assumed that consumers can participate in DRPs based on incentive payment. The proposed price package and the amount of demand reduction are used to run these programs.

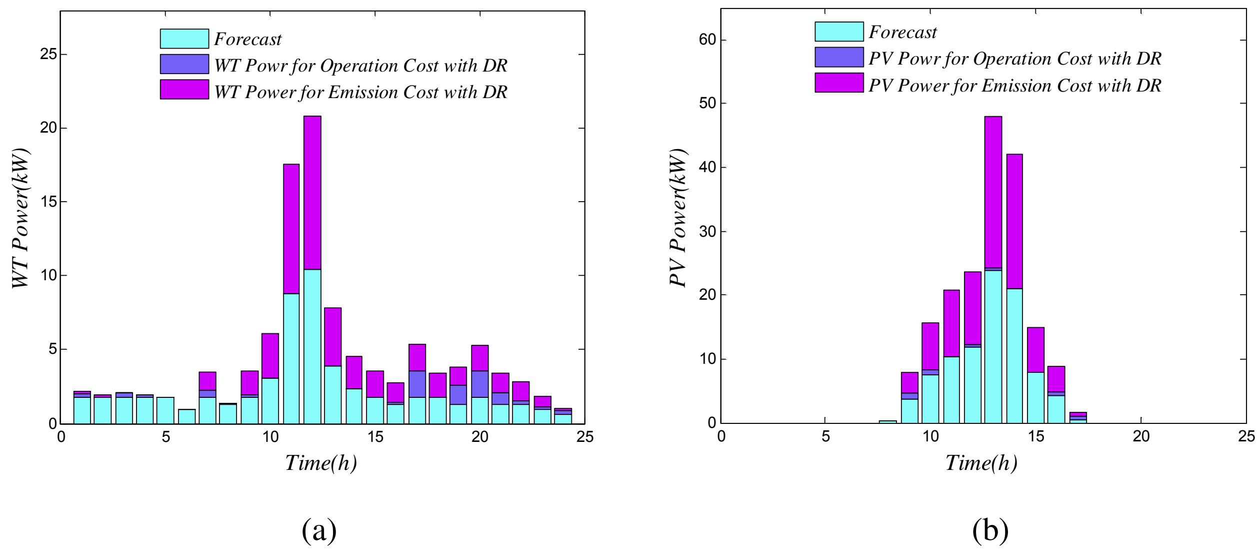

Fig. 13. Output power (a) Wind turbine (b) Solar cell, considering operating cost and emission with DR.

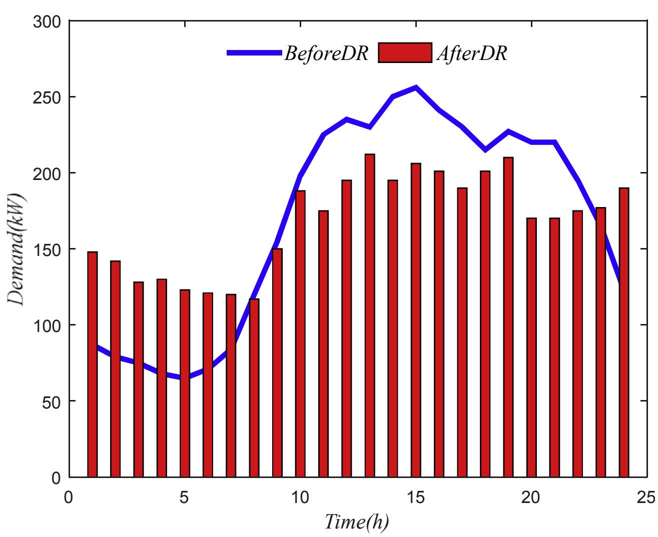

Fig. 14. Load demand before and after DR implementation.

The MOPSO method, based on fuzzy techniques, was used to solve the proposed model and achieve an optimal response.

The results of the simulations showed that if consumers participate in DRPs, there is a possibility for reducing the operational costs and emissions. Among the studied cases, simultaneous consideration of operational costs and pollution emissions, with the involvement of DR, produced the best results by reducing operational cost and pollution emissions by 21% and 14%, respectively. In addition, results of the simulation showed that considering the pollution function as the main objective, it increased the operational costs such that maximum use of demand response programs occurred in this case, compared with the operating condition. Another important result is providing a model with a simple structure. As this model shows, if consumers participate in demand response, in addition to covering the production shortages caused by the uncertainty derived from wind and solar power, this will result in a reduction of operating costs and the system's overall pollution.

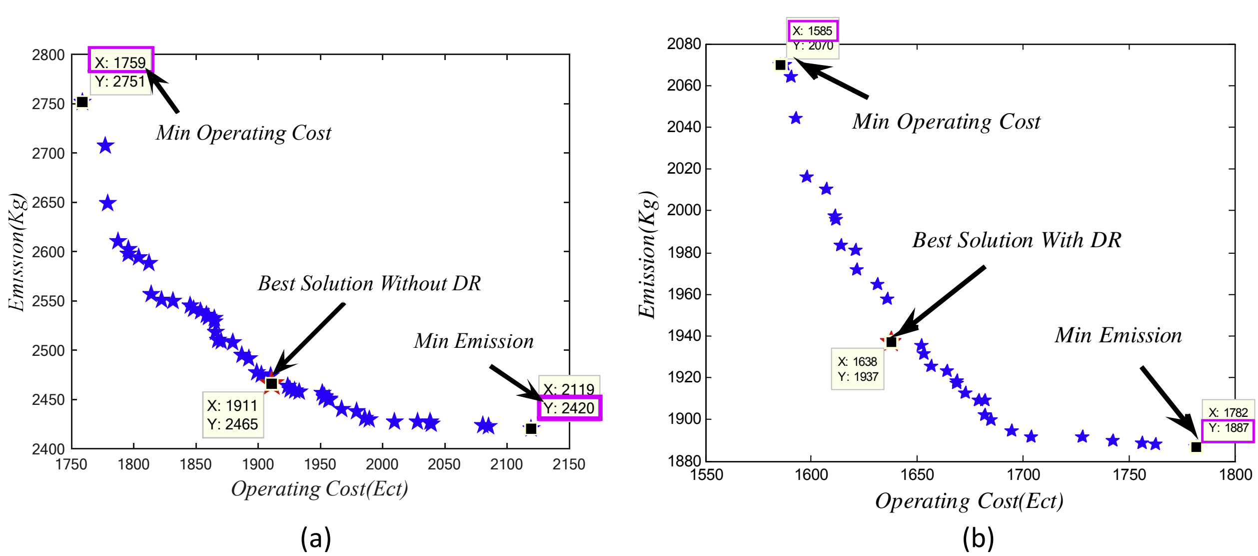

Fig. 15. Pareto criterion for operating costs and pollution (a) without DR (b) with DR.

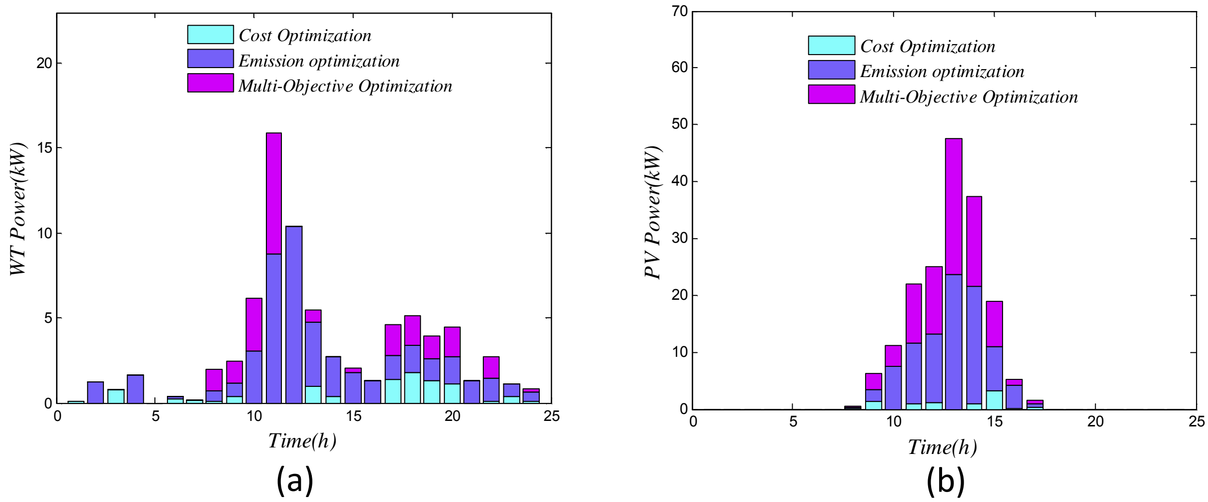

Fig. 16. Power generation (a) Wind turbine (b) Solar cell.

Table 7
Comparison of solar and wind generation capacity from the perspective of operating costs and emissions without/with DR.

Cases	Wind power (kW)	Solar power (kW)	Wind power forecast (kW)	Solar power forecast (kW)	Cover percentage of wind power	Cover percentage of solar power
Operating costs without DR	8.51	4.82	57.15	91.47		
Operating costs with DR	7.87	3.34	57.15	91.47	**7.5%**	**30.7%**
Emissions without DR	50.605	91.39	57.15	91.47		
Emissions with DR	47.39	89.50	57.15	91.47	6.3%	2.1%
Simultaneous optimization without DR	23.12	90.21	57.15	91.47		
Simultaneous optimization without DR	21.97	78.27	57.15	91.47	4.9%	13.2%

Operating costs with DR are written in bold.

References

[1] Sun Q, Ge X, Liu L, Xu X, Zhang Y, Niu R, et al. Review of smart grid comprehensive assessment systems. Energy Procedia 2011;12:219–29.
[2] Mazlumi K. Presenting a new method based on branch placement for optimal placement of phasor measurement units. J Operation Automation Power Eng 2014;2(2):113–20.
[3] Colak I, Kabalci E, Fulli G, Lazarou S. A survey on the contributions of power electronics to smart grid systems. Renew Sustain Energy Rev 2015;47:562–79.
[4] López G, Moreno J, Amarís H, Salazar F. Paving the road toward Smart Grids through large-scale advanced metering infrastructures. Electr Power Syst Res 2015;120:194–205.
[5] A survey on advanced metering infrastructure and its application in Smart Grids. In: Mohassel RR, Fung AS, Mohammadi F, Raahemifar K, editors. 2014 IEEE 27th canadian conference on. Electrical and Computer Engineering (CCECE); 2014.
[6] Bouhafs F, Mackay M, Merabti M. Communication challenges and solutions in the smart grid. Springer; 2014.
[7] Verma PK, Sharma H. Application of cloud computing In Smart grid: a review. International conference of advance research and innovation (ICARI-2015); 404–409.
[8] Vardakas JS, Zorba N, Verikoukis CV. Performance evaluation of power demand scheduling scenarios in a smart grid environment. Appl Energy 2015;142:164–78.
[9] Albadi MH, El-Saadany E. A summary of demand response in electricity markets. Electr Power Syst Res 2008;78(11):1989–96.
[10] Khan AA, Razzaq S, Khan A, Khursheed F. HEMSs and enabled demand response in electricity market: an overview. Renew Sustain Energy Rev 2015;42:773–85.
[11] Alavi SA, Ahmadian A, Aliakbar-Golkar M. Optimal probabilistic energy management in a typical micro-grid based-on robust optimization and point estimate method. Energy Convers Manag 2015;95:314–25.
[12] Zakariazadeh A, Jadid S, Siano P. Stochastic multi-objective operational planning of smart distribution systems considering demand response programs. Electr Power Syst Res 2014;111:156–68.
[13] Zakariazadeh A, Jadid S, Siano P. Economic-environmental energy and reserve scheduling of smart distribution systems: a multiobjective mathematical programming approach. Energy Convers Manag 2014;78:151–64.
[14] Mohamed FA, Koivo HN. System modelling and online optimal management of microgrid using mesh adaptive direct search. Int J Electr Power & Energy Syst 2010;32(5):398–407.
[15] Rezaei N, Kalantar M. Smart microgrid hierarchical frequency control ancillary service provision based on virtual inertia concept: an integrated demand response and droop controlled distributed generation framework. Energy Convers Manag 2015;92:287–301.
[16] Cicek N, Delic H. Demand response management for smart grids with wind power. IEEE transactions on. Sustain Energy 2015;6(2):625–34.
[17] Afshar K, Gazafroudi AS. Application of stochastic programming to determine operating reserves with considering wind and load uncertainties. J Operation Automation Power Eng 2013;1(2):96–109.
[18] Rahimi E, Rabiee A, Aghaei J, Muttaqi KM, Nezhad AE. On the management of wind power intermittency. Renew Sustain Energy Rev 2013;28:643–53.
[19] Gen B. Reliability and cost/worth evaluation of generating systems utilizing wind and solar energy. 2005.
[20] Owner's manual of the AIR403 wind turbine made by Southwest Wind power Inc. www.nooutage.com/pdf/swwp_air403_landman.pdf.
[21] Abouzahr I, Ramakumar R. An approach to assess the performance of utility-interactive wind electric conversion systems. Energy Conversion. IEEE Trans 1991;6(4):627–38.
[22] Atwa Y, El-Saadany E, Salama M, Seethapathy R. Optimal renewable resources mix for distribution system energy loss minimization.,IEEE Transactions on. Power Syst 2010;25(1):360–70.
[23] Ettoumi FY, Mefti A, Adane A, Bouroubi M. Statistical analysis of solar measurements in Algeria using beta distributions. Renew Energy 2002;26(1):47–67.
[24] Deshmukh M, Deshmukh S. Modeling of hybrid renewable energy systems. Renew Sustain Energy Rev 2008;12(1):235–49.
[25] Tina G, Gagliano S, Raiti S. Hybrid solar/wind power system probabilistic modelling for long-term performance assessment. Sol Energy 2006;80(5):578–88.
[26] Chowdhury S, Crossley P. Microgrids and active distribution networks. The Institution of Engineering and Technology; 2009.
[27] Mazzola S, Astolfi M, Macchi E. A detailed model for the optimal management of a multigood microgrid. Appl Energy 2015;154:862–73.
[28] Kanchev H, Lu D, Colas F, Lazarov V, Francois B. Energy management and

operational planning of a microgrid with a PV-based active generator for smart grid applications. IEEE Transactions on. Ind Electron 2011;58(10):4583–92.
[29] Moghaddam AA, Seifi A, Niknam T, Pahlavani MRA. Multi-objective operation management of a renewable MG (micro-grid) with back-up micro-turbine/fuel cell/battery hybrid power source. Energy 2011;36(11):6490–507.
[30] Kennedy J. Particle swarm optimization. Encyclopedia of machine learning. Springer; 2010. p. 760–6.
[31] MOPSO: a proposal for multiple objective particle swarm optimization. In: Coello Coello CA, Lechuga MS, editors. Evolutionary computation, 2002 CEC'02 proceedings of the 2002 congress on; 2002.
[32] A benchmark low voltage microgrid network. In: Papathanassiou S, Hatziargyriou N, Strunz K, editors. Proceedings of the CIGRE Symposium: power systems with dispersed generation; 2005.
[33] Apx power spot exchange. Accessted at, https://www.apxgroup.com/trading-clearing/apx-power-uk/.
[34] Bouffard F, Galiana FD, Conejo AJ. Market-clearing with stochastic security-part I: formulation. IEEE Transactions on. Power Syst 2005;20(4):1818–26.
[35] Willy Weather. Available online: http://wind.willyweather.com.au.
[36] The Solar Power Group Company. Accessed at, http://thesolarpowergroup.com.au.
[37] Reconstruction and Short-term Forecast of the Solar Irradiance. Accessed at, http://lpc2e.cnrs-orleans.fr/~soteria/.
[38] Bouhouras AS, Labridis DP, Bakirtzis AG. Cost/worth assessment of reliability improvement in distribution networks by means of artificial intelligence. Int J Electr Power & Energy Syst 2010;32(5):530–8.
[39] Chen C, Duan S, Cai T, Liu B, Hu G. Smart energy management system for optimal microgrid economic operation. IET Renew power Gener 2011;5(3):258–67.
[40] Clement-Nyns K, Haesen E, Driesen J. The impact of charging plug-in hybrid electric vehicles on a residential distribution grid. IEEE Transactions Power Syst 2010;25(1):371–80.
[41] Staff F. Assessment of demand response and advanced metering. Docket AD-06-2-000. Federal Energy Regulatory Commission; 2006.